Anal Bioanal Chem (2017) 409:1827–1836
DOI 10.1007/s00216-016-0127-3

RESEARCH PAPER

SPRi-MALDI MS: characterization and identification of a kinase from cell lysate by specific interaction with different designed ankyrin repeat proteins

Ulrike Anders[1] · Jonas V. Schaefer[2] · Fatima-Ezzahra Hibti[3] · Chiraz Frydman[3] · Detlev Suckau[4] · Andreas Plückthun[2] · Renato Zenobi[1]

Received: 28 September 2016 / Revised: 22 November 2016 / Accepted: 29 November 2016 / Published online: 16 December 2016

Abstract We report on the direct coupling of surface plasmon resonance imaging (SPRi) with matrix-assisted laser desorption/ionization mass spectrometry (MALDI MS) for the investigation of specific, non-covalent interactions, using the example of designed ankyrin repeat proteins (DARPins) and ribosomal protein S6 kinase 2 (RPS6KA2) directly from lysate of SH-SY5Y cells, derived from human bone marrow. Due to an array format, tracing of binding kinetics of numerous DARPins simultaneously and in real time becomes possible. By optimizing both the proteolytic digest directly on the SPRi chip (amount of trypsin, incubation time, and temperature) as well as the MALDI matrix application (concentration of matrix and number of spray cycles), we are able to identify the specific interaction with RPS6KA2 directly from the cell lysate at a surface coverage of only 0.8 fmol/mm^2.

Keywords Surface plasmon resonance imaging (SPRi) · MALDI mass spectrometry · Designed ankyrin repeat proteins (DAPRins) · Cell lysate · Label-free

Electronic supplementary material The online version of this article (doi:10.1007/s00216-016-0127-3) contains supplementary material, which is available to authorized users.

✉ Renato Zenobi
zenobi@org.chem.ethz.ch

[1] Department of Chemistry and Applied Biosciences, ETH Zurich, Vladimir-Prelog-Weg 3, 8093 Zurich, Switzerland

[2] Department of Biochemistry, University of Zurich, Winterthurerstrasse 190, 8057 Zurich, Switzerland

[3] Horiba Jobin Yvon S.A.S., Avenue de la Vauve-Passage Jobin Yvon, CS 45002, 91120 Palaiseau, France

[4] Bruker Daltonics, Fahrenheitstr. 4, 28359 Bremen, Germany

Introduction

In pharmaceutical and life science research, there is an increasing demand for methods that provide both kinetic and thermodynamic characterization of biomolecular interactions, ideally combined with quantification and unambiguous identification of the respective binding partners. For affinity reagents like antibodies or alternative binding scaffolds, information about their affinity as well as their off-target specificity/cross-reactivity are essential to identify the best suited lead candidates. However, to obtain all this information, it is generally necessary to employ more than one analytical method, which makes the whole procedure elaborate and time-consuming. To tackle this challenge, Nelson and coworkers already successfully combined surface plasmon resonance (SPR) with mass spectrometry in the late 1990s [1–3]. The first technology allows the analysis of non-covalent interactions of biomolecules in a label-free fashion and provides information on binding kinetics (k_{on}/k_{off}) from which equilibrium constants (K_A, K_D) can be derived. Binding affinities can be monitored in real time by this sensitive method, allowing the detection of interacting partners in the femtomole range. If a chip set-up is used, working in an SPR array format can provide rapid and high-throughput analysis of different interactions in parallel. One drawback of SPR, however, is the unknown identity of the interacting species since only the increase in mass is detected, but not the nature of the causative agent. In contrast, matrix-assisted laser desorption/ionization mass spectrometry (MALDI MS) can characterize the ligands captured on an SPR chip surface and thus identify them on the molecular level, based on their molecular weight and peptide fingerprints.

Originally, SPR and MALDI MS analyses were performed separately [4–15], which presented a serious limitation of the workflow, as micro-recovery procedures were needed to elute

captured ligands. This was often associated with sample loss and contamination, resulting in rather large amounts of sample being required for unambiguous sample identification. Thus, it became obvious that MALDI MS analyses directly on the chip would be a major improvement and of clear advantage. The benefits of such an approach were demonstrated in several well-conducted studies [15–24]. However, these analyses were mostly performed on commercial SPR surfaces [25, 26] that had only a single target analyte present on the chip, thereby severely limiting the throughput of such measurements.

Our aim was therefore to develop a hyphenated SPR-MALDI strategy that employs patterned SPR chips and would thus enable multiplexing—a promising analytical strategy which has not yet been deeply explored in this context [27–30]. To allow multiplexing and thus the analysis of numerous samples in parallel, we utilized the SPR imaging technology [27], benefitting from the spatial resolution capabilities of imaging by visualizing the whole SPR biochip with a high-resolution CCD camera. In the present study, we choose designed ankyrin repeat proteins (DARPin) as binders [31], which already showed their specificity to their respective target in the past, but had not yet been used for such a multiplexing experiment.

To be broadly applicable and to allow versatile operations, the intended platform was designed to investigate not only pure target solutions but also complex mixtures like cellular lysates. As in the past either pure or spiked samples were used [24, 29], such nonbiased biological samples have not been studied in depth. As one of the few examples, Musso and coworkers [30] chose human saliva as the analyte solution to detect α-amylase, a major human enzyme. However, SPRi-MALDI MS has never been performed with cell lysates as established in the presented platform and shown here. To enhance the final mass spectra, we further optimized the tryptic digest (see below) to take place without generating any potentially interfering autolysis peaks in the spectra. This improvement clearly facilitated and increased the quality of the recorded mass spectra tremendously with respect to the low amounts of captured analyte (low fmol range) from the cell lysate. A scheme of the SPRi-MALDI MS workflow used in this work is shown in Fig. 1.

Here, we describe the measurement of specific binding as well as the analysis of potential off-target binding of various DARPins against the ribosomal protein S6 kinase 2. DARPins are a very promising class of non-immunoglobulin binders that rival antibodies for target recognition and have been used

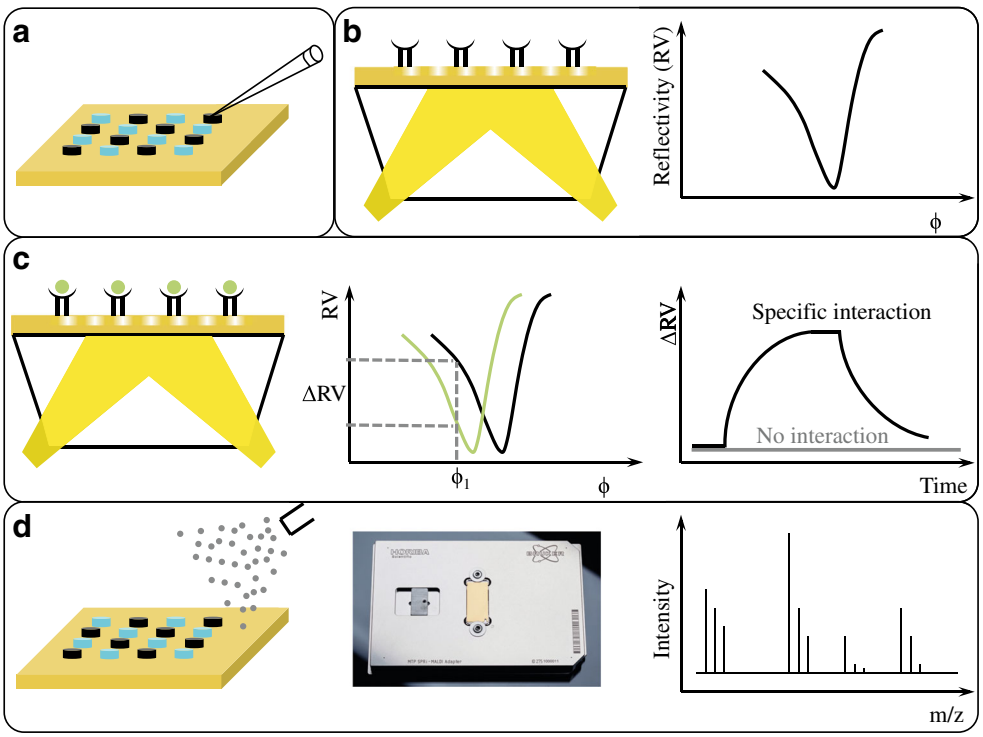

Fig. 1 Scheme of the SPRi measurement followed by MALDI matrix application and MALDI MS measurement. **a** Ligands of interest are spotted and covalently immobilized on the chip by NHS ester chemistry. **b** The prepared slide is inserted in the flow cell of the SPR instrument and the surface plasmon resonance (SPR) curve is generated. **c** The injected analyte solution covers the whole surface. Interactions on the surface will change the SPR curve. The difference in reflectivity (ΔRV) is recorded and used to generate a sensorgram where specific interactions can be followed (*right graph*). This is performed simultaneously for each spot on the surface. **d** After SPRi analysis, the gold slide is removed from the instrument and a MALDI matrix is deposited with an airbrush. Prior to matrix deposition, an on-chip tryptic digestion can be performed optionally by spraying a trypsin solution on the chip. For identification of the captured proteins, the gold slide is mounted on an adapter and inserted into the mass spectrometer

in a variety of applications, ranging from basic research to improved diagnostics to therapeutic applications [31, 32]. Having a relatively small size and being very stable repeat proteins, DARPins are more robust than antibodies and can also easily be tagged for oriented chemical coupling to solid supports by various means. Importantly and in contrast to antibody-derived binders, DARPins predominantly bind to structural (three-dimensional) rather than linear epitopes and thus allow recognition of their respective targets with very high specificities and sensitivities. The target of the selected DARPins in this study (RPS6KA2) belongs to a family of serine/threonine protein kinases and has been implicated in cell cycle progression [33] as well as being a presumed actor for tumor suppression in ovarian cancer [34]. Furthermore, RPS6KA2 was recently identified as a potential drug target and seems to be suitable for the development of novel inhibitors for pancreatic cancer therapy [35].

In the past, the coupling of SPRi to MALDI MS was challenging, in particular to identify an optimum procedure for matrix application and for enzymatic digestion in a very small volume directly on the chip surface. In addition, most prior studies were conducted with purified, recombinantly expressed target proteins rather than with "real-world" samples. These issues are addressed experimentally in the present work, and an optimized workflow for obtaining reliable results is presented.

Materials and methods

Chemicals and reagents

Acetonitrile (Chromasolv for HPLC >99.9%), mouse IgG (technical grade) (used as negative control), bovine serum albumin (BSA, >98.0%), hydrochloric acid (HCl, puriss. p.a. >37.0%), trifluoroacetic acid (TFA, >99.0% for protein sequencing), potassium chloride (KCl, puriss. p.a. >99.5%), and α-cyano-4-hydroxycinnamic acid (α-CHCA, matrix substance for MALDI MS, >99.0%) were purchased from Sigma-Aldrich. Sequencing Grade Modified Trypsin and Trypsin Gold (mass spectrometry grade) were ordered from Promega. Acetic acid sodium salt anhydrous (>99.0%), sodium phosphate dibasic (Na_2HPO_4, for analysis 98.5%), and glycine (>99.0%) came from Acros. Ethanolamine (puriss. p.a. >99.0%), ammonium bicarbonate (BioUltra, >99.5%), and sinapinic acid (matrix substance for MALDI MS, >99.0%) were obtained from Fluka. Tryptic digest of bovine serum albumin (polypeptide fragment mixture for testing MALDI-TOF MS) was purchased from CARE, Bruker Daltonics. Formic acid (98–100% for analysis), sodium chloride (NaCl, for analysis), and potassium dihydrogen phosphate (KH_2PO_4, for analysis) were ordered from Merck.

The kinase domain of RPS6KA2 (UniProt identifier Q15349) was expressed and kindly provided by Dr. Susanne Müller-Knapp from the SGC Oxford and the DARPins 243_C05, 113_D02, 276_C08, and 244_A07 were selected and produced by the High-Throughput Binder Selection Facility (HT-BSF) of the University of Zurich. The cell lysate of SH-SY5Y was kindly provided by Chia-Lung Yang from the group of Prof. Olga Shakhova (Department of Oncology, University Hospital Zurich).

All buffers were prepared using ultrapure water (MilliQ water, 18.2 MΩ cm^{-1}).

Surface plasmon resonance imaging

The gold slides used during the experiments were purchased from Horiba Jobin Yvon (France) and were already functionalized with a self-assembled monolayer of polyoxyethylene carrying an N-hydroxy succinimide (NHS) ester group for direct use. DARPins were coupled via their surface lysine residues to the NHS ester.

For this purpose, 0.3 μL of a 0.1 mg/mL protein solution (DARPins: 243_C05, 113_D02, 276_C08, 244_A07 (based on internal nomenclature)) were spotted in triplicates on the chip. The spot array pattern used here was a 4 × 4 mask, but in principle, up to 20 × 20 spots could be arrayed simultaneously. Aqueous sodium acetate (10 mM, pH 5) was used as immobilization buffer. The spotted droplets were kept in a humid atmosphere for 1 h in a cooled ultrasonic cleaner and then washed with MilliQ water. For blocking the remaining free ester groups, the surface was immersed in 1 M aqueous ethanolamine for 15 min on a vibrating plate. Afterwards, the slide was washed with water and a regeneration solution (100 mM aqueous glycine adjusted with HCl to pH 2) was added for an additional 15 min on a vibrating plate to allow all non-covalently bound ligands to dissociate.

The washed and dried gold slide was attached to a glass prism with a high refractive index via a thin film of index-matching oil (2.8 μL were sufficient to cover the entire surface). SPRi experiments were performed in PBS buffer (137 mM NaCl, 2.7 mM KCl, 10 mM Na_2HPO_4, 1.8 mM KH_2PO_4, pH 7.4) at a flow rate of 50 μL/min using a 200 μL sample injection loop at room temperature. Runs were performed for 12 min, with 3 min for the association and 9 min for the dissociation step. Dilutions of the injected target protein solutions were prepared with the same solutions used as running buffers. By injecting 100 mM glycine in HCl (pH 2) or only aqueous formic acid (pH 2), it was possible to regenerate the gold slide to start a new binding step.

For SPRi measurements, a commercial instrument was used (SPRi-Plex II from Horiba Jobin Yvon, Palaiseau, France). It is based on intensity modulation and uses a high-stability light-emitting diode (LED) and a charge-coupled device (CCD) camera to measure the reflectivity variation

(%RV) at a fixed angle. This can be converted into captured analyte quantities per surface unit (0.02% RV refers to 3.7 pg/mm^2). The optical setup is based on the Kretschmann configuration [36], where a high refractive index glass prism is used as resonance coupler.

The measured kinetic curves were evaluated with the instrument software (SPRiAnalysis 2.3.1). Calculations of the binding constants, k_{on}, k_{off}, K_D, were done with the Scrubber Gen2 software, using a 1:1 model (BioLogic Software Pty Ltd, GenOptics Version). Standard deviations given were calculated from triplicate measurements that were globally fitted.

MALDI MS

MALDI MS was either done on the intact protein or on a tryptic digest thereof produced directly on the chip surface. For the latter, the gold slide was removed from the SPRi instrument and air-dried. To perform an on-chip tryptic digest, 0.3 μL of a 5 ng/μL trypsin solution in 10 mM ammonium bicarbonate (pH 8.3) was dropped on the region of interest. The gold chip was kept in a humid atmosphere at 37 °C for 10 min. The spots were dried at 37 °C to stop the digestion. For matrix application, the slide was put inside a closed box with only a small hole for the nozzle of an airbrush. The solutions were then nebulized with a gentle stream of N_2 at 0.8 bar with an airbrush for deposition on the chip. Therefore, the slide was held at a distance of 24 cm from the airbrush. At the beginning, 1 mL of aqueous TFA (0.1%) was sprayed to create a humid atmosphere followed by the α-CHCA matrix (7 mg/mL in 50% acetonitrile/water with 0.3% TFA).

For analyzing the intact proteins, the slide was also put inside the box mentioned above and 1 mL of 0.2% aqueous TFA was sprayed. The acidic environment served to dissociate non-covalent bonds between surface-bound ligand and analyte. Subsequently, 1 mL aliquots of a 10 mg/mL sinapinic acid solution in 50% acetonitrile/water with 0.3% TFA were sprayed ten times, always followed by a drying time to avoid spot coalescence on the chip surface. The matrix was dried under ambient conditions.

Mass spectra were acquired with an Ultraflex II MALDI-TOF (Bruker Daltonics, Bremen, Germany) with the gold slide mounted to the SPRi-MALDI adapter target. The mass spectrometer was equipped with a "smartbeam" laser working with a 66.7 Hz repetition rate. Spectra were acquired in linear positive ion mode for intact proteins with an accelerating voltage of 25 kV and pulsed ion extraction of 150 ns. The laser fluency was attenuated to just above the desorption/ionization threshold. Peptide spectra were acquired in reflective positive ion mode with an accelerating voltage of 25 kV and pulsed ion extraction of 20 ns. Again, laser fluency was attenuated to just above the desorption/ionization threshold. Each mass spectrum was the average of 1500–2000 laser shots acquired at random sample positions. All mass spectra were smoothed, baseline-subtracted, and externally calibrated with the standard peptide calibration mix I (LaserBio Labs), spotted on the SPRi chip with an expected mass accuracy of about 20–50 ppm. Tryptic peptides were identified with the Biotools software (Bruker Daltonics) and Mascot software (Matrix Science Limited). Adducts (e.g., Cu^{2+}) were computationally removed prior to a Mascot database search.

Results

Interaction of DARPins with RPS6KA2

In the past, we already performed selection of DARPins against the kinase domain of RPS6KA2 (unpublished). From the resulting dozens of specific hits, we choose three candidates (113_D02, 243_C05, and 276_C08), which all had high affinities, but are very different in the sequence composition of their interacting paratopes and therefore partly bind to different epitopes on their target as detected by epitope binning experiments (unpublished). In addition, throughout our investigations we used DARPin 244_A07 (not binding to RPS6KA2) as a negative control for all performed assays. In the present study, we analyzed the specific non-covalent interaction between the DARPins and RPS6KA2 by the arrayed SPRi-MALDI MS slides (shown in Fig. 2b as image of the flow cell). After immobilizing the DARPins via accessible lysines on their surface to the NHS moieties on the chip and injecting several concentrations of the kinase domain of RPS6KA2 (5–40 nM, with regeneration steps in between), kinetic curves were recorded and the dissociation constants (K_D) determined (see Table 1). Kinetic curves for 243_C05 and 113_D02 are shown in Fig. 2a as these two DARPins differ the most towards the specific interaction to the target. In Fig. 2c, the signal level at the end of the association phase (mean value) for every DARPin and for every concentration was plotted. Standard deviations given reflect the variation between the triplicate measurements of the immobilized DARPin, which were found to be in good agreement. To visualize specific interactions, the SPRi image recorded upon injection of RPS6KA2 could be used (difference image shown in Fig. 2b). The SPR data clearly show that the strongest interaction is between RPS6KA2 and binders 243_C05 or 276_C08 (see Electronic Supplementary Material (ESM) Fig. S1 for kinetic curve), respectively, followed by DARPin 113_D02. A specific interaction to 244_A07 could not be observed (ESM Fig. S2)—and thus this DARPin was employed throughout the study as a negative control. It should be noted that the curves do not reach saturation, which is a consequence of the high binder concentration immobilized. This may lead to mass-transport limitations and rebinding phenomena, such that the kinetic constants and K_D determined

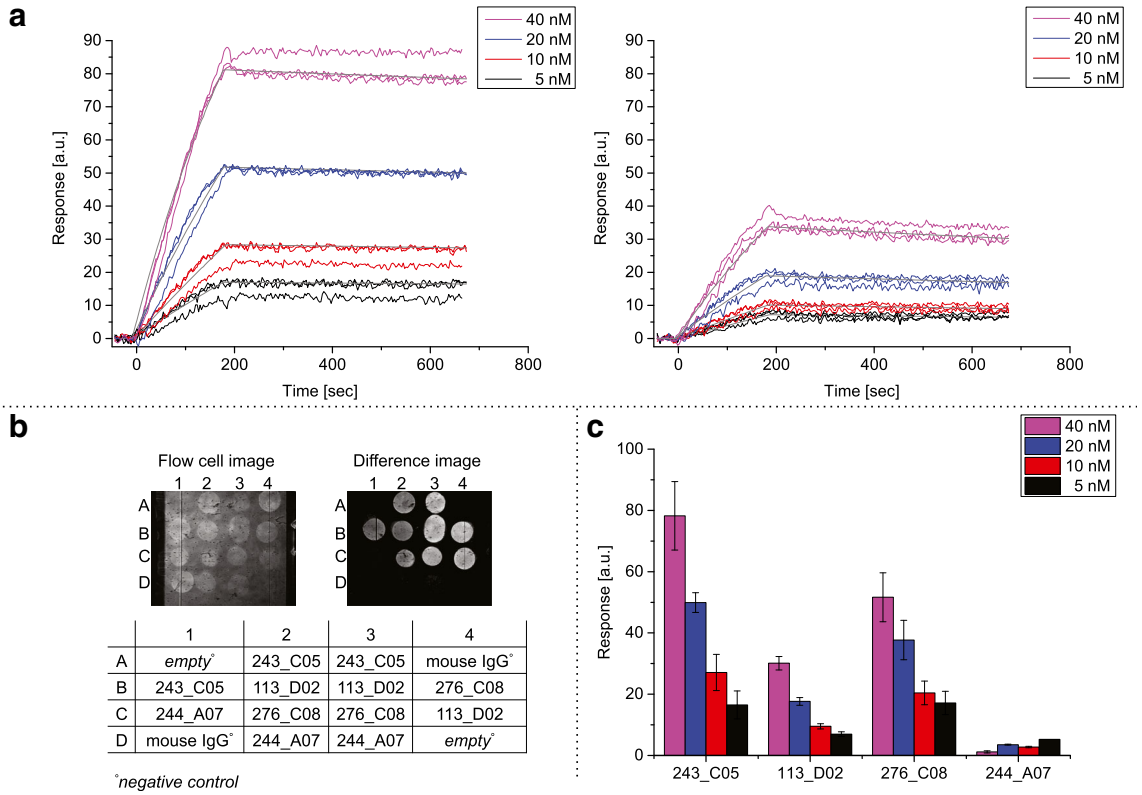

Fig. 2 SPRi measurements for four DARPins with a concentration series of RPS6KA2. **a** Kinetic curves for 243_C05 (*left*) and 113_D02 (*right*) with a concentration series of RPS6KA2. K_D values of 0.52 ± 0.01 nM for 243_C05 and 4.5 ± 0.1 nM for 113_D02 were calculated (*fitted curves shown in gray*). **b** SPRi flow cell image of the arrayed SPRi-MALDI MS slide (*left*) and SPRi difference image recorded upon injection of RPS6KA2 (*right*). **c** Mean values of signal level of the end of the association phase with standard deviation for every DARPin and injected concentration (5–40 nM)

may not be accurate, an issue warranting further detailed investigations.

After SPRi analysis of RPS6KA2 (without regenerating the surface), the slide was directly submitted to on-chip MALDI MS analysis. The resulting mass spectrum (Fig. 3) is comparable to the spectrum of the purified kinase domain of RPS6KA2 (having a theoretical molecular weight = 41,448.10 Da) obtained separately by a standard MALDI MS measurement. The mass shift of circa 200 *m/z* of the measured value compared to the theoretical one could be caused by matrix adducts, as it is known that sinapinic acid tends to form +206 Da adducts with the analyte ions [37]. The mass spectrum shown in Fig. 3 originates from a spot where 243_C05 was immobilized, and measurements on the spots of the other target-binding DARPins, 113_D02 as well as 276_C08, gave similar results (ESM Fig. S6). It was also verified that RPS6KA2 signals were not detectable in the negative control (mouse IgG), nor on empty spots (no immobilized protein), nor on the non-binding control DARPin 244_A07 spot. This result confirms the ability of our set-up to efficiently detect captured specific binding partners on the SPRi chip surface.

Table 1 Association and dissociation rate constants and K_Ds for several DARPins interacting with the target protein RPS6KA2. Standard deviations reflect measurements on triplicates of the immobilized DARPin and global fitting

DARPin	k_{on} (M^{-1} s^{-1})	k_{off} (s^{-1})	K_D
243_C05	$1.51 \pm 0.01 \times 10^5$	$7.8 \pm 0.2 \times 10^{-5}$	0.52 nM (±0.01 nM)
276_C08	$1.70 \pm 0.02 \times 10^5$	$9.9 \pm 0.2 \times 10^{-5}$	0.58 nM (±0.01 nM)
113_D02	$5.3 \pm 0.2 \times 10^4$	$2.36 \pm 0.04 \times 10^{-4}$	4.5 nM (±0.1 nM)

To identify the affinity-captured RPS6KA2 not only by its molecular weight (not easily observed because of the low intensity of the captured intact protein) but also by the peptide mass fingerprint (PMF), we subsequently performed a tryptic digest directly on the chip. The resulting peptides were analyzed by MALDI MS (Fig. 4) and identified with the Biotools software and a Mascot database search. Based on the tryptic peptide ions listed in Table 2, the PMF analysis led to a clear identification of RPS6KA2 at only 5.6 fmol/mm^2 (eight fragments, 12.3% sequence coverage, 52.0% intensity coverage, Mascot score 89). PMF mass spectra for the remaining two specific interacting DARPins, 113_D02 and 276_C08, showed similar results and are shown in the ESM in Fig. S7/

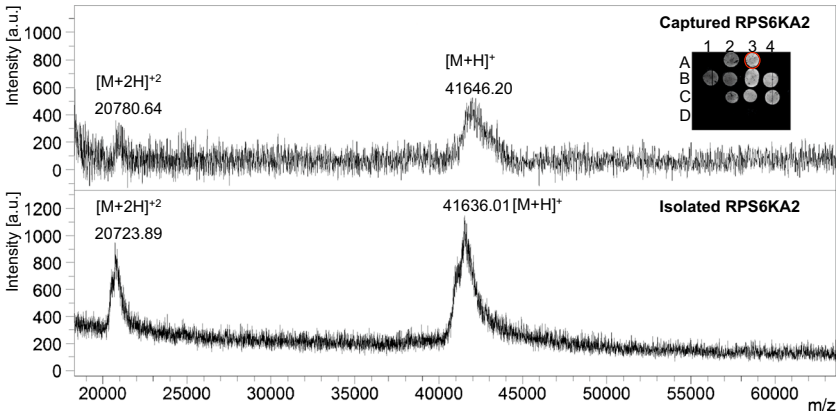

Fig. 3 *Top*, on-chip MALDI mass spectrum of intact RPS6KA2 captured by the immobilized DARPin 243_C05 on the SPRi gold slide on spot A3 (SPRi difference image same as shown in Fig. **2b**); *bottom*, standard MALDI mass spectrum of RPS6KA2 (50 fmol) measured on a pure gold slide

Table S2 and Fig. S8/Table S3, respectively. It should be noted that peptides of RPS6KA2 could neither be detected on the spots of the control DARPin 244_A07 (no SPR signal) nor on the negative control areas (ESM Figs. S9 and S10).

As mentioned in the "Introduction", enzymatic digestion in a very small volume directly on the chip surface is rather challenging. Using high amounts of trypsin (e.g., 50–90 ng/μL) as published previously [28, 30, 38], strong peaks of autolysis fragments disrupt recorded mass spectra. Therefore, we adapted the amount of trypsin to tenfold lower concentrations for an optimal digestion efficiency to prevent the formation of autolysis peptides (Fig. 4) that had been seen in prior work [30]. Furthermore, the MALDI matrix application procedure turned out to be crucial for the quality of the mass spectra. When the matrix was spotted from a solution with high acetonitrile content, drops were spreading, thus increasing the spot size and therefore analyte dilution and spot-to-spot cross-contamination. In contrast, by spraying the matrix with an airbrush (see "Materials and methods"), a very homogenous distribution without any "coffee ring effects" or cross-contamination could be achieved, and multiplexed investigations became possible. To determine optimal conditions for matrix application and tryptic digestion, we performed preliminary studies with BSA and a commercially available tryptic digest of BSA, respectively. For this purpose, we investigated the concentration of α-cyano-4-hydroxycinnamic-acid (α-CHCA), number of spray cycles, and solvent on one hand, and incubation time, amount as well as trypsin specification and temperature for optimal digestion on the other hand. These results are summarized in ESM Fig. S14 and Fig. S15. The optimal conditions identified are described in the section "Materials and methods".

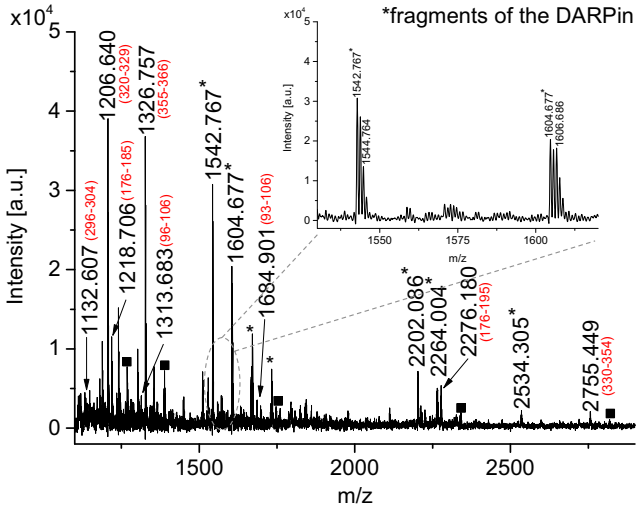

Fig. 4 On-chip MALDI mass spectrum after SPRi measurement and on-chip proteolysis of captured RPS6KA2 retained on 243_C05. Fragments of RPS6KA2 are labeled with their sequence range and Cu^{2+}-adducts are marked with *black box*. Peptides of the DARPin 243_C05 are marked with an *asterisk*

As listed in Table 2, Cu^{2+}-adducts ($[M + Cu^{2+}-H^+]^+$) of most detected peptides were also observed. Copper has two stable isotopes (^{63}Cu, 70% and ^{65}Cu, 30%), which leads to a characteristic isotopic pattern (zoomed part in the upper right corner of Fig. 4). Laser ablation inductively coupled plasma mass spectrometry (LA-ICP-MS) measurements made clear that copper originated from the SPRi chip itself (data not shown). The presence of these signals results in a reduced sensitivity of the performed measurements. Due to Cu^{2+}-adducts, almost twice as many peaks of the digested DARPin were detected, which in turn could suppress fragments of the target protein.

Cell lysate

As mentioned before, the purified RPS6KA2 used in this study and for the generation of the DARPin binders was not of full length, but consisted only of its kinase domain. While the confirmed interaction of the binders with this construct might suggest a similar recognition of the full-length protein, a direct proof would be important for the further development of these binders since some epitopes might be blocked in the full-length variant. Fortunately, the hyphenated SPRi-MALDI platform is well suited to investigate not only pure target solutions but also complex mixtures. Therefore, we used a lysate of the cell line SH-SY5Y, derived from human bone marrow,

Table 2 Peptide mass fingerprint of on-chip digested captured RPS6KA2 retained on 243_C05 after SPRi measurement (*fragments of the DARPin 243_C05). Cu^{2+}-adducts are mentioned in parentheses

Meas. *m/z*	Theor. *m/z*	|Δ ppm|	Seq. range	Sequence
1132.607	1132.568	34.4	296–304	MLHVDPHQR
1206.640 (1268.581)	1206.611 (1268.633)	24.0 (41.0)	320–329	EYLSPNQLSR (Cu^{2+}-adduct)
1218.706	1218.684	18.1	176–185	DLKPSNILYR
1313.683	1313.695	9.1	96–106	DPSEEIEILLR
1326.757 (1388.658)	1326.738 (1388.659)	14.3 (0.7)	355–366	LEPVLSSNLAQR (Cu^{2+}-adduct)
1684.901 (1746.835)	1684.923 (1746.845)	13.1 (5.7)	93–106	SKRDPSEEIEILLR (Cu^{2+}-adduct)
2276.180 (2338.122)	2276.158 (2338.074)	9.7 (20.5)	176–195	DLKPSNILYRDESGSPESIR (Cu^{2+}-adduct)
2755.449 (2817.394)	2755.446 (2817.368)	1.1 (9.2)	330–354	QDVHLVKGAMAATYFALNRTPQAPR (Cu^{2+}-adduct)
1542.767 (1604.677)	1542.787 (1604.709)	13.0 (19.9)	18–31	LLEAARAGQDDEVR* (Cu^{2+}-adduct)
1670.743 (1732.703)	1670.882 (1732.504)	35.3 (22.5)	17–31	KLLEAARAGQDDEVR* (Cu^{2+}-adduct)
2202.086 (2264.004)	2202.092 (2264.014)	2.7 (4.4)	148–167	TPFDLAIDNGNEDIAEVLQK* (Cu^{2+}-adduct)
2534.305	2534.277	11.0	145–167	FGKTPFDLAIDNGNEDIAEVLGK*

that is known to contain high levels of RPS6KA2 according to the Human Protein Atlas [39].

For this experiment, the DARPins (243_C05, 113_D02, 276_C08, and 244_A07) were again immobilized on the gold slide and a concentration series of a diluted SH-SY5Y cell lysate (1:4,150 to 1:33,300) was injected. In Fig. 5 (right side), mean values of the signal level of the end of the association phase for every DARPin and every concentration were plotted. Interactions were recorded on three different spots for each DARPin. The measured kinetic curves were in good agreement among different spots of the same DARPin, as shown by the fairly low standard deviations. When comparing the sensorgram for 243_C05 from pure RPS6KA2 (Fig. 2a left side) with that of the SH-SY5Y cell lysate containing RPS6KA2 (Fig. 5 left side), no major differences are detectable. The calculated dissociation constant of $K_D = 0.43 \pm 0.01$ nM is in the range of the experimental accuracy and fitting deviations as that for pure RPS6KA2. The other two DARPins (113_D02 and 276_C08) behaved in a same way. Both DARPins showed a similarly strong specific interaction as with pure RPS6KA2 (see ESM for kinetic curves (Figs. S3–S5) and K_Ds (Table S1)).

After injecting the least diluted (i.e., the most highly concentrated) solution of SH-SY5Y lysate (1:4,150), the slide was removed from the SPR instrument and a tryptic digest was directly performed on the chip. The proteolytic peptides were subsequently detected by MALDI MS (Fig. 6) and identified using the Biotools software and Mascot software. The peptide ions at $m/z = 1206.637$, 1218.714, 1326.742, 1684.937, and 2755.449 (and their Cu^{2+}-adducts) represent the measured peptide mass fingerprint of RPS6KA2, which is therefore clearly identified from only as little as 0.8 fmol/mm^2 (five fragments, 9.7% sequence coverage, 46.4% intensity coverage, Mascot score 67). Additional ions detected were the same as shown in Fig. 4 and belong to the DARPin 243_C05. Again, no autolysis of trypsin was detected. PMF

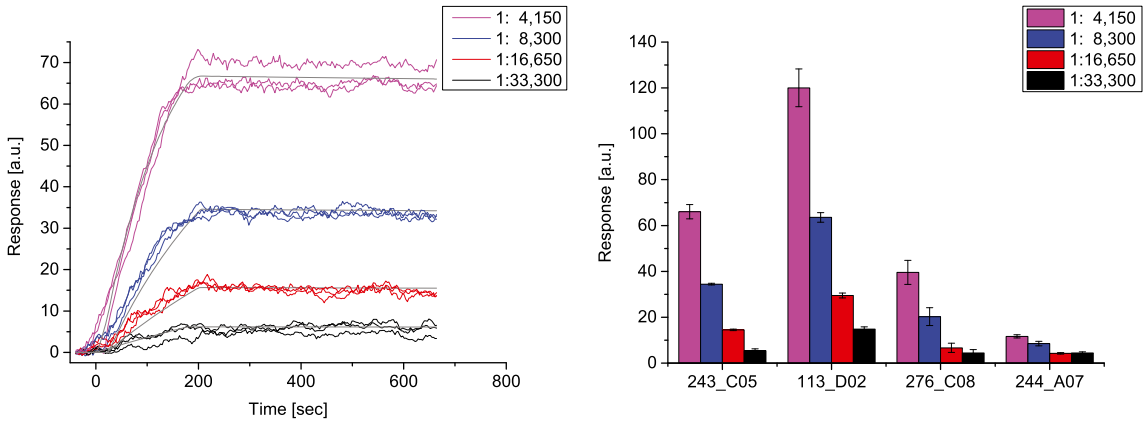

Fig. 5 SPRi measurements for four different DARPins with a concentration series of SH-SY5Y. *Left*, kinetic curves for 243_C05 with a concentration series of SH-SY5Y. A K_D value of 0.43 ± 0.01 nM was calculated (*fitted curves shown in gray*). *Right*, mean values of signal level of the end of the association phase with standard deviation for every DARPin and injected dilution (1:33,300–1:4,150)

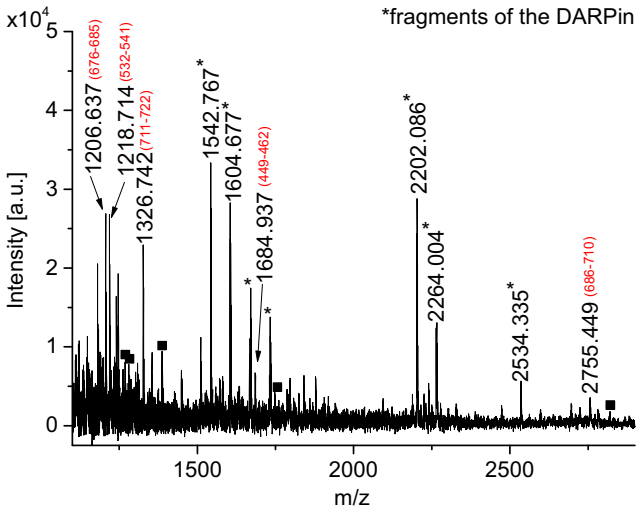

Fig. 6 On-chip MALDI mass spectrum after SPRi measurement and on-chip tryptic digestion of captured RPS6KA2 (from SH-SY5Y) retained on 243_C05. Fragments of RPS6KA2 are labeled with its sequence range and Cu^{2+}-adducts are marked with *black square*. Peptides of the DARPin 243_C05 are marked with an *asterisk*

mass spectra for the remaining DARPins, 113_D02 and 276_C08, showed analogous results and are summarized in the ESM in Fig. S11/Table S4 and Fig. S12/Table S5, respectively. Again the control DARPin 244_A07 showed no SPR signal and no peptides could be identified (ESM Fig. S13).

Discussion

Here, we demonstrate for the first time the suitability of SPRi-MALDI MS coupling to follow binding affinities and to identify the target molecules of immobilized affinity reagents directly in a lysate of a cell line (SH-SY5Y), derived from human bone marrow. Results obtained are similar to those from purified proteins or from spiking of crude extracts—the more traditional approaches. By optimizing the amount of trypsin such that the tryptic proteolysis still worked reliably and efficiently, but without any interfering autolysis fragments, the recorded mass spectra were cleaner and peptides of interest easier to identify than in previous studies [30]. By *spraying* instead of *spotting* the MALDI matrix, we further overcame the problem of drops spreading even if the matrix solution has a high acetonitrile content. The sprayed matrix proved to be homogenously distributed without any "coffee ring effects" or cross-contamination. As a consequence, this optimized SPRi-MALDI MS workflow performed reliably and resulted in improved signals. Using this method, we analyzed different previously selected DARPins and determined their affinities to their respective target RPS6KA2 in mammalian cell lysates, which turned out to be almost identical to the values derived from measurements with purified protein. Furthermore, we also confirmed the specificity of the binders and the identity of the specific target (RPS6KA2) in this cell lysate at low femtomole levels.

Being able to detect specific protein-protein interactions and to measure the affinities in crude extracts instead of using purified proteins obviously has numerous advantages. For recombinant protein production for target generation, it is often easier as well as less time- and cost-intensive to express these proteins in *Escherichia coli* rather than in mammalian cell culture, and in addition, to focus on defined domains, rather than full-length proteins with all unstructured regions (as it also was the case for the kinase domain of RPS6KA2 used in this study). Even though every target undergoes quality control for being folded before selections are started, some proteins are post-translationally modified in the original eukaryotic host, e.g., by phosphorylation for intracellular proteins or glycosylation for extracellular proteins. It is therefore essential to validate that the selected binders recognize the full-length target in the natural cellular environment, ideally already during the initial screening. Thus, being able to screen a rather large number of binders simultaneously for their interaction with intracellular proteins directly in cell lysates via the here established SPRi-MALDI MS workflow could be a major improvement for binder screening and validation analyses. Although only four different DARPins were analyzed simultaneously in this study, upscaling to hundreds of individual candidates should be feasible [40–43] and is planned for future projects. In addition to upscaling for higher throughput, further improvements with regard to the formation of Cu^{2+}-adducts with a refined SPRi chip surfaces should be possible. An automation of ligand spotting or an automated spray technology to increase array density and to get a better reproducibility could also be pursued. Related to the few tryptic fragments of the target analyte (RPS6KA2) detected with MALDI MS, it could be considered for future investigations to improve the proteolytic digestion, e.g., by reduction prior to the addition of the enzyme to counteract air-catalyzed on-chip oxidation.

While we still plan to improve and refine this method, the newly established workflow already now provides rapid answers to the question whether the recognized epitopes are accessible in the cellular context or potentially blocked by other intracellular interaction partners, provided that such an interaction would survive the generation of the cell lysate and that the interaction partner is present in at least stoichiometric amounts. In addition, the experimental set-up will also allow analyzing affinity reagents for off-target binding and cross-reactivities in the real biological context, namely in the cellular environment. Because the bound ligands, i.e., the target proteins, can be identified based on the recorded fragments and the subsequent assignment to peptide sequences through database matching, first indications about the specificity of the affinity reagents can be obtained by using this method. Generating all this information in a single assay should clearly speed up the identification of lead candidates from binder

libraries and thus will make the whole process of binder generation both faster and less resource-intensive.

Acknowledgements We thank Horiba Jobin Yvon for the loan of an SPRi instrument and Bruker Daltonics and Horiba Jobin Yvon for jointly funding 1.5 years of a Ph.D. studentship awarded to U.A. We also thank all current and former members of the High-Throughput Binder Selection Facility for their contribution to the establishment of the semi-automated ribosome display that resulted in the used DARPin binders. The RPS6KA2 target used for DARPin selection and the experiments described here was kindly provided by Dr. Susanne Müller-Knapp and Tracy Keates (SGC Oxford). Chia-Lung Yang (group of Prof. Olga Shakhova) kindly provided the cell lysate of SH-SY5Y (Department of Oncology, University Hospital Zurich).

Compliance with ethical standards

Conflict of interest The authors declare that they have no conflict of interest.

References

1. Krone JR, Nelson RW, Dogruel D, Williams P, Granzow R. BIA/MS: interfacing biomolecular interaction analysis with mass spectrometry. Anal Biochem. 1997;244(1):124–32. doi:10.1006/abio.1996.9871.
2. Nelson RW, Krone JR, Jansson O. Surface plasmon resonance biomolecular interaction analysis mass spectrometry. 1. Chip-based analysis. Anal Chem. 1997;69(21):4363–8. doi:10.1021/ac970538w.
3. Nelson RW, Krone JR. Advances in surface plasmon resonance biomolecular interaction analysis mass spectrometry (BIA/MS). J Mol Recognit. 1999;12(2):77–93. doi:10.1002/(SICI)1099-1352(199903/04)12:2<77::AID-JMR448>3.0.CO;2-G.
4. Sönksen CP, Nordhoff E, Jansson Ö, Malmqvist M, Roepstorff P. Combining MALDI mass spectrometry and biomolecular interaction analysis using a biomolecular interaction analysis instrument. Anal Chem. 1998;70(13):2731–6. doi:10.1021/ac9800457.
5. Natsume T, Nakayama H, Jansson Ö, Isobe T, Takio K, Mikoshiba K. Combination of biomolecular interaction analysis and mass spectrometric amino acid sequencing. Anal Chem. 2000;72(17):4193–8. doi:10.1021/ac000167a.
6. Mattei B, Cervone F, Roepstorff P. The interaction between endopolygalacturonase from *Fusarium moniliforme* and PGIP from *Phaseolus vulgaris* studied by surface plasmon resonance and mass spectrometry. Comp Funct Genom. 2001;2:359–64. doi:10.1002/cfg.113.
7. Lopez F, Pichereaux C, Burlet-Schiltz O, Pradayrol L, Monsarrat B, Estève J-P. Improved sensitivity of biomolecular interaction analysis mass spectrometry for the identification of interacting molecules. Proteomics. 2003;3(4):402–12. doi:10.1002/pmic.200390055.
8. Catimel B, Rothacker J, Catimel J, Faux M, Ross J, Connolly L, et al. Biosensor-based micro-affinity purification for the proteomic analysis of protein complexes. J Proteome Res. 2005;4(5):1646–56. doi:10.1021/pr050132x.
9. Larsericsdotter H, Jansson Ö, Zhukov A, Areskoug D, Oscarsson S, Buijs J. Optimizing the surface plasmon resonance/mass spectrometry interface for functional proteomics applications: how to avoid and utilize nonspecific adsorption. Proteomics. 2006;6(8):2355–64. doi:10.1002/pmic.200401353.
10. Bouffartigues E, Leh H, Anger-Leroy M, Rimsky S, Buckle M. Rapid coupling of surface plasmon resonance (SPR and SPRi) and ProteinChip™ based mass spectrometry for the identification of proteins in nucleoprotein interactions. Nucleic Acids Res. 2007;35(6):e39-e. doi:10.1093/nar/gkm030.
11. Visser NFC, Scholten A, van den Heuvel RHH, Heck AJR. Surface-plasmon-resonance-based chemical proteomics: efficient specific extraction and semiquantitative identification of cyclic nucleotide-binding proteins from cellular lysates by using a combination of surface plasmon resonance, sequential elution and liquid chromatography–tandem mass spectrometry. ChemBioChem. 2007;8(3):298–305. doi:10.1002/cbic.200600449.
12. Hayano T, Yamauchi Y, Asano K, Tsujimura T, Hashimoto S, Isobe T, et al. Automated SPR-LC–MS/MS system for protein interaction analysis. J Proteome Res. 2008;7(9):4183–90. doi:10.1021/pr700834n.
13. Marchesini GR, Buijs J, Haasnoot W, Hooijerink D, Jansson O, Nielen MWF. Nanoscale affinity chip interface for coupling inhibition SPR immunosensor screening with nano-LC TOF MS. Anal Chem. 2008;80(4):1159–68. doi:10.1021/ac071564p.
14. Stigter ECA, de Jong GJ, van Bennekom WP. Development of an on-line SPR-digestion-nanoLC-MS/MS system for the quantification and identification of interferon-γ in plasma. Biosens Bioelectron. 2009;24(7):2184–90. doi:10.1016/j.bios.2008.11.020.
15. Treitz G, Gronewold TMA, Quandt E, Zabe-Kühn M. Combination of a SAW-biosensor with MALDI mass spectrometric analysis. Biosens Bioelectron. 2008;23(10):1496–502. doi:10.1016/j.bios.2008.01.013.
16. Nedelkov D, Nelson RW. Practical considerations in BIA/MS: optimizing the biosensor–mass spectrometry interface. J Mol Recognit. 2000;13(3):140–5. doi:10.1002/1099-1352(200005/06)13:3<140::AID-JMR496>3.0.CO;2-P.
17. Nedelkov D, Nelson RW. Exploring the limit of detection in biomolecular interaction analysis mass spectrometry (BIA/MS): detection of attomole amounts of native proteins present in complex biological mixtures. Anal Chim Acta. 2000;423(1):1–7. doi:10.1016/S0003-2670(00)01077-1.
18. Nelson RW, Nedelkov D, Tubbs KA. Biomolecular interaction analysis mass spectrometry. Anal Chem. 2000;72(11):404 A–11. doi:10.1021/ac0028402 .
19. Nelson RW, Nedelkov D, Tubbs KA. Biosensor chip mass spectrometry: a chip-based proteomics approach. Electrophoresis. 2000;21(6):1155–63. doi:10.1002/(SICI)1522-2683(20000401)21:6<1155::AID-ELPS1155>3.0.CO;2-X.
20. Nedelkov D, Nelson RW. Analysis of native proteins from biological fluids by biomolecular interaction analysis mass spectrometry (BIA/MS): exploring the limit of detection, identification of nonspecific binding and detection of multi-protein complexes. Biosens Bioelectron. 2001;16(9–12):1071–8. doi:10.1016/S0956-5663(01)00229-9.
21. Grote J, Dankbar N, Gedig E, Koenig S. Surface plasmon resonance/mass spectrometry interface. Anal Chem. 2005;77(4):1157–62. doi:10.1021/ac049033d.
22. Nedelkov D, Tubbs KA, Nelson RW. Surface plasmon resonance-enabled mass spectrometry arrays. Electrophoresis. 2006;27(18):3671–5. doi:10.1002/elps.200600065.
23. Boireau W, Rouleau A, Lucchi G, Ducoroy P. Revisited BIA-MS combination: entire "on-a-chip" processing leading to the proteins identification at low femtomole to sub-femtomole levels. Biosens Bioelectron. 2009;24(5):1121–7. doi:10.1016/j.bios.2008.06.030.
24. Rouleau A, Osta M, Lucchi G, Ducoroy P, Boireau W. Immuno-MALDI-MS in human plasma and on-chip biomarker characterizations at the femtomole level. Sensors. 2012;12(11):15119.

25. Vassilios IA. Surface plasmon resonance (SPR) and ELISA methods for antibody determinations as tools for therapeutic monitoring of patients with acute lymphoblastic leukemia (ALL) after native or pegylated *Escherichia coli* and *Erwinia chrysanthemi* asparaginases. Biosensors and Molecular Technologies for Cancer Diagnostics. Series in Sensors: Taylor & Francis; 2012. p. 89–108.
26. Schlensog MD, Gronewold TMA, Tewes M, Famulok M, Quandt E. A Love-wave biosensor using nucleic acids as ligands. Sensor Actuat B-Chem. 2004;101(3):308–15. doi:10.1016/j.snb.2004.03.015.
27. Nedelkov D. Development of surface plasmon resonance mass spectrometry array platform. Anal Chem. 2007;79(15):5987–90. doi:10.1021/ac070608r.
28. Bellon S, Buchmann W, Gonnet F, Jarroux N, Anger-Leroy M, Guillonneau F, et al. Hyphenation of surface plasmon resonance imaging to matrix-assisted laser desorption ionization mass spectrometry by on-chip mass spectrometry and tandem mass spectrometry analysis. Anal Chem. 2009;81(18):7695–702. doi:10.1021/ac901140m.
29. Remy-Martin F, El Osta M, Lucchi G, Zeggari R, Leblois T, Bellon S, et al. Surface plasmon resonance imaging in arrays coupled with mass spectrometry (SUPRA–MS): proof of concept of on-chip characterization of a potential breast cancer marker in human plasma. Anal Bioanal Chem. 2012;404(2):423–32. doi:10.1007/s00216-012-6130-4.
30. Musso J, Buchmann W, Gonnet F, Jarroux N, Bellon S, Frydman C, et al. Biomarkers probed in saliva by surface plasmon resonance imaging coupled to matrix-assisted laser desorption/ionization mass spectrometry in array format. Anal Bioanal Chem. 2015;407(5):1285–94. doi:10.1007/s00216-014-8373-8.
31. Plückthun A. Designed ankyrin repeat proteins (DARPins): binding proteins for research, diagnostics, and therapy. Annu Rev Pharmacool Toxicol. 2015;55(1):489–511. doi:10.1146/annurev-pharmtox-010611-134654.
32. Boersma YL, Plückthun A. DARPins and other repeat protein scaffolds: advances in engineering and applications. Curr Opin Biotechnol. 2011;22(6):849–57. doi:10.1016/j.copbio.2011.06.004.
33. Pancholi S, Lykkesfeldt AE, Hilmi C, Banerjee S, Leary A, Drury S, et al. ERBB2 influences the subcellular localization of the estrogen receptor in tamoxifen-resistant MCF-7 cells leading to the activation of AKT and RPS6KA2. Endocr-Relat Cancer. 2008;15(4):985–1002. doi:10.1677/erc-07-0240.
34. Bignone PA, Lee KY, Liu Y, Emilion G, Finch J, Soosay AER et al. RPS6KA2, a putative tumour suppressor gene at 6q27 in sporadic epithelial ovarian cancer. Oncogene. 2006;26(5):683–700. http://www.nature.com/onc/journal/v26/n5/suppinfo/1209827s1.html.
35. Milosevic N, Kühnemuth B, Mühlberg L, Ripka S, Griesmann H, Lölkes C, et al. Synthetic lethality screen identifies RPS6KA2 as modifier of epidermal growth factor receptor activity in pancreatic cancer. Neoplasia. 2013;15(12):1354–62. doi:10.1593/neo.131660.
36. Kretschmann E. Decay of non radiative surface plasmons into light on rough silver films. Comparison of experimental and theoretical results. Opt Commun. 1972;6(2):185–7. doi:10.1016/0030-4018(72)90224-6.
37. Beavis RC, Chait BT, Fales HM. Cinnamic acid derivatives as matrices for ultraviolet laser desorption mass spectrometry of proteins. Rapid Commun Mass Spectrom. 1989;3(12):432–5. doi:10.1002/rcm.1290031207.
38. Forest S, Breault-Turcot J, Chaurand P, Masson J-F. Surface plasmon resonance imaging-MALDI-TOF imaging mass spectrometry of thin tissue sections. Anal Chem. 2016;88(4):2072–9. doi:10.1021/acs.analchem.5b03309.
39. Human Protein Atlas. http://www.proteinatlas.org/ENSG00000071242-RPS6KA2/cell. Accessed 08.08.2016 2016.
40. Wang W, Fang Q, Hu Z. High-throughput peptide screening on a bimodal imprinting chip through MS-SPRi integration. In: Cretich M, Chiari M, editors. Peptide Microarrays: Methods and Protocols. New York, NY: Springer New York; 2016. p. 111–25.
41. Ritorto MS, Ewan R, Perez-Oliva AB, Knebel A, Buhrlage SJ, Wightman M et al. Screening of DUB activity and specificity by MALDI-TOF mass spectrometry. Nat Commun. 2014;5. doi:10.1038/ncomms5763
42. Haslam C, Hellicar J, Dunn A, Fuetterer A, Hardy N, Marshall P, et al. The evolution of MALDI-TOF mass spectrometry toward ultra-high-throughput screening: 1536-well format and beyond. J Biomol Screen. 2016;21(2):176–86. doi:10.1177/1087057115608605.
43. Lee JH, Choi HS, Nasr KA, Ha M, Kim Y, Frangioni JV. High-throughput small molecule identification using MALDI-TOF and a nanolayered substrate. Anal Chem. 2011;83(13):5283–9. doi:10.1021/ac2006735.